Complete Local Spatial Relationship Pattern: An Efficient Texture Feature Descriptor for Image Retrieval

Chelladurai Callins Christiyana *, Murugesan Poomani Punitha **

** Department of Computer Science and Engineering, SRM Madurai College for Engineering and Technology, Madurai, Tamilnadu, India (callinschristiyanac@gmail.com)*
*** Department of Information Technology, Sethu Institute of Technology, Virudhunagar, Tamilnadu, India (punithapoomani@gmail.com)*

Abstract: Texture is an exemplary feature widely used to characterize images in content-based image retrieval (CBIR) approaches. Local pattern-based texture features show significant promise in representing image characteristics, as they are computationally efficient and highly discriminative for retrieving similar images. This article proposes a new local pattern, the Complete Local Spatial Relationship Pattern (CLSRP), for texture representation in image retrieval. Unlike other local patterns, CLSRP partitions neighbouring pixels based on spatial distance and assigns corresponding weights during encoding. It comprehensively characterizes texture by incorporating the magnitude and sign components of neighbourhood relationships, along with center pixel binary mapping relative to a global threshold. CLSRP's effectiveness is experimentally validated on two standard databases, ORL and UIUC, and a real-world COVID-19 chest X-ray database, using precision and recall as evaluation metrics. Quantitative results show CLSRP achieves average precision scores of 0.81, 0.72, and 0.91 on the ORL, UIUC, and COVID-19 datasets, respectively, outperforming state-of-the-art local pattern-based methods (LTriDP, LNIP, LBP) by up to 18–29%, confirming its robustness and superior retrieval effectiveness.

Keywords: Feature extraction, Local Pattern, Image database, Image texture analysis, Pattern formation, Pattern matching, Image Retrieval.

1. INTRODUCTION

The generation of electronic images multiplies exponentially with the extensive use of digital gadgets and the internet in human life. These images are stored and are used effectively in fields, including medicine, education, and media. Similar images of an interesting one from the image collection are often obtained and referred to with the help of image retrieval (IR) techniques. CBIR is the most efficient IR technique and retrieves alike images from the image collection according to the visual likeness of the images (Liua et al., 2007; Zhang et al., 2012). Visual likeness among the images is determined with the help of primitive features such as shape, colour and texture inherent in the images (Tian, 2013).

The texture is the pivotal feature of an image, and is utilised to represent one, ranging from microscopic to multi-band images. The texture feature is extensively used in analyzing visual data in a remarkable accuracy as it perceives the images similar to human perception (Liu, 2019). Various texture representation methods are used in image retrieval applications. Gray level co-occurrence matrix (GLCM) (Haralick et al., 1973), Tamura features (Tamura et al., 1978), Wavelet coefficients (Loupias et al., 2000), Ridgelets and Curvelets (Sumana et al., 2008), Gabor wavelet filter (Manjunath and Ma, 1996), Gray level histogram, edge histogram, and local binary pattern (LBP) (Ojala et al., 1996) are some of the premier approaches of texture characterization.

The LBP texture representation is a unique operator that blends the structural and statistical approaches. On account of its characteristics like simple to compute, computationally efficient, and illumination invariant, LBP is employed for image analysis in difficult real-world contexts like medical image evaluation, facial recognition, and motion analysis. Numerous LBP variants are being generated for texture representation.

1.1 Review of LBP Variants

(Jin et al., 2004) presented an ILBP - Improved Local Binary Patterns to represent facial images. The average gray intensity in the local neighbourhood has been used for encoding in ILBP, because it reflects both local shape and texture information. The authors have concluded that ILBP is illumination invariant for discriminating facial images.

A Median Binary Pattern (MBP) for texture classification was developed by (Hafiane et al., 2007). MBP thresholds the gray-scale values of every pixel in the local neighbourhood with respect to the median value. The authors have validated that MBP performs better when compared to LBP for texture classification in the Outex database.

(Heikkila et al., 2009) presented Center-Symmetric Local Binary Patterns (CSLBP) to observe identical images and group the similar objects. In contrast to the LBP, CSLBP utilised center symmetric relationships to derive the local pattern. The authors have shown that the CSLBP pattern is robust on flat image areas and produces a shorter length histogram than LBP.

(Liao et al., 2009) contributed the DLEP - Dominant Local Binary Pattern to classify the textures. DLBP makes use of the recurring patterns to apprehend interpretive textural details. The authors have demonstrated that DLBP achieves higher classification accuracy in different texture databases and under different imaging conditions.

(Tan and Triggs, 2010) introduced LTP- Local Ternary Patterns for face image representation. LTP employs ternary thresholding and generates two binary patterns from the same local neighbourhood. The authors have demonstrated that LTP is more discriminative than LBP and exhibits greater robustness to noise in homogeneous regions.

(Guo et al., 2010) developed CLBP-Completed Local Binary Patterns for texture classification. The CLBP is the composite of CLBP_M, CLBP_S and CLBP_C. CLBP_S is the binary pattern, derived by considering the sign of differences between the gray values, and CLBP_M is the binary pattern, derived by considering the absolute distinctions of the gray values. CLBP_C is the result of binary thresholding of the gray value of the center pixel and the average gray value of the entire image. The efficacy of CLBP has been validated on the Outex and CUReT databases.

(Nanni et al., 2010) presented Elongated Quinary Patterns (EQP) for extracting texture features from medical images. They employed five levels of encoding within an elliptic-shaped neighbourhood to derive EQP. Experimental results have demonstrated that EQP outperforms LBP and LTP in the categorization of medical image features.

(Zhang et al., 2010) designed LDP-Local Derivative Pattern to recognize and verify face images. LDP derives higher-order local information from the specified region by recording its diverse characteristic spatial relationships. The FERET, CAS-PEAL, CMU-PIE, Extended Yale B, and FRGC databases have been experimented by the authors. They have demonstrated that, in a variety of scenarios, higher order LDP outperforms LBP in both face verification and identification.

(He and Sang, 2011) introduced Gradient Local Binary Patterns (GLBP). While LBP performs well under standard illumination variations, GLBP is rotation invariant and demonstrates robust performance in texture analysis under reflective lighting conditions. The authors have illustrated the efficacy of GLBP under obscure illumination conditions.

(Qian et al., 2011) presented a PLBP- Pyramid Transform Domain Local Binary Pattern for classifying textures. PLBP descriptors acquire texture resolution variations as a factor and are turned into multi-resolution LBP.

(Murala et al., 2012a) developed a DLEP - Directional Local Extrema Pattern for retrieving images based on content. Each pixel in the neighbourhood uses center symmetric relationships to derive the DLEP patterns in the 0◦, 45◦, 90◦, and 135◦ directions. The authors have illustrated the significant improvement of DLBP over LBP and CSLBP in the Corel and Brodatz databases.

(Murala et al., 2012b) modeled the LMEBP - Local Maximum Edge Binary Pattern for object tracking and image retrieval. LMEBP uses maximum edges to extract information from the neighbourhood. The image retrieval experiments have been carried out on the Brodatz and MIT Vistex databases. Based on comparisons with LBP and LTP, the authors have demonstrated a notable improvement in LMEBP’s performance.

(Murala et al., 2012c) contributed the LTrP - Local Tetra Pattern to retrieve the images based on its contents. LTrP uses the first-order derivatives in the 0◦ and 90◦ directions to represent the relationship between the referenced pixel and its neighbours. The magnitude and sign components of LTrP are used to represent image features. The retrieval accuracy of the image retrieval systems in the Corel and Brodatz databases has demonstrated the effectiveness of LTrP in comparison with LBP, LDP, and LTP.

(Reddy and Reddy, 2014) extended the DLEP by integrating the magnitudes of Local Extrema. The authors represented the image using both the sign and magnitude components of DLEP. They carried out experiments on the Corel 5k and Corel 10k databases, and have concluded that DLEP with magnitude patterns produced better image retrieval accuracy than DLEP, LBP, and CSLBP.

(Xia et al., 2014) presented LSBP - Local Spatial Binary Patterns for the image retrieval process. In order to determine the pattern, LSBP accounts the spatial distribution information of gray level variation in the local neighbourhood. The retrieval performance of LSBP has been compared against that of LBP, LTP, CLBP, and LTrP in the Brodatz, MIT VisTex, and Corel databases. The authors have concluded that LSBP performs well, when compared with LBP.

(Verma and Raman, 2015) conceived a CSLBCoP - Center Symmetric Local Binary Co-occurrence Pattern for retrieving similar images from a database. The image is used to create the CSLBP pattern map, which provides local information. Gray Level Co-occurrence Matrices (GLCMs) are employed to capture pixel-pair co-occurrence in multiple directions and distances. The resulting GLCMs are aggregated to generate the final image feature vector. Experimental validation on medical, face, and texture image datasets has demonstrated that pixel-pair co-occurrence provides greater reliability than pattern frequency.

(Dubey et al., 2015) introduced Local Diagonal Extrema Patterns (LDEP) for medical image retrieval applications. The LDEP descriptor is encoded using local diagonal minima and maximas derived from the central pixel and its neighbouring diagonal pixels. Compared to alternative methods for CT image retrieval, LDEP achieves the fastest retrieval performance.

(Christiyana and Rajamani, 2015) introduced the CLSCDBP - Complete Local Spatial Central Derivative Binary Pattern for ultrasound kidney image retrieval. The mutual relationships between the neighbours at various spatial distances are taken into account by the CLSCDBP pattern. The global mean statistics are also included in CLSCDBP to make the pattern complete. The authors have demonstrated a significant improvement in the retrieval accuracy of ultrasound kidney images with the CLSCDBP pattern.

(Verma and Raman, 2016) presented the LTriDP - Local Tri-Directional Pattern for image retrieval applications. For image feature representation, the sign and magnitude components of the pattern which are obtained from the local intensity of pixels depending on three directions in the neighbourhood are utilised. The authors have experimented the capability of the LTriDP in texture and face databases and have deduced that the LTriP outstrips the compatible patterns for image retrieval applications.

(Verma and Raman, 2017) formulated the LNDP - Local Neighbourhood Difference Pattern for image retrieval. The mutual associations among the neighbouring pixels in the local neighbourhood serve as the foundation for devising the LNDP. The authors combined LNDP with LBP and performed image retrieval on the natural and texture image databases. Compared to other local patterns, they have demonstrated a notable increase in the retrieval accuracy of the combined LNDP and LBP characteristics.

The LNIP - Local Neighbourhood Intensity Pattern was developed by (Banerjee et al., 2018) for content-based image retrieval. Both sign and magnitude components present in the LNIP pattern. The relationship between every neighbouring pixel with its surrounding pixels is the conception of the LNIP pattern. After conducting tests in the Brodatz, MIT VisTex, Salzburg, and AT&T databases, the authors have concluded that LNIP performs better in terms of retrieval accuracy than other local approaches.

(Sukhia et al., 2020) presented image retrieval techniques for remote sensing images using multi-scale local ternary patterns. The image is down sampled in three scales using this method. LTP pattern is extracted from each down sampled image. The authors have demonstrated the effectiveness of multi-scale local ternary patterns on the 21-class land cover dataset and the 20-class satellite remote sensing dataset.

(Xu et al., 2020) formulated a CLSP - Completed Local Shrinkage Pattern for classifying the textures. They hve demonstrated that CLSP attained a high trade-off between discernment and dimensionality. In addition to the local neighbourhood encoding, center pixel encoding is also done to make the local pattern complete. The authors have conducted experiments in four benchmark databases and have demonstrated the superior classification performance of the CSLP.

An enhanced LTP was introduced by (Fekri and Ershad, 2020) to categorize the bark texture photos. The improved LTP is uniformly labeled, and the feature vector of the image is formed using the labels occurrence probability. The authors have demonstrated that the improved LTP provides noise resistance and rotationally invariant behaviours in addition to improved classification accuracy.

The multi-level directional cross-binary patterns were formed by (Kas et al., 2020) to categorize texture images. The pattern is encoded using the multiple radius neighbourhoods. They have used a multi-level directional cross binary pattern to show how to recognize gray level variations that happen in different directions.

An Optimized Local Weber and Gradient Pattern (OLWGP)-based image retrieval and classification model for medical images was presented by (Mahesh et al., 2021). The advantages of both the LGP and the differential excitation component of LWP are combined in OLWGP. The authors have validated the effectiveness of the OLWGP pattern with LBP, LDP, LGP, LWP and showed OLWGP attained higher retrieval accuracy.

(Pan et al., 2021) used an Adaptive Center Pixel Selection (ACPS) technique to handle the issue of recovering degraded texture information from non-uniform binary patterns. The Outex, UIUC, CUReT, XU_HR, ALOT, and KTHTIPS2b databases have been used in the experimentation. In comparison to LBP and its variations, the authors have concluded that the ACPS approach greatly increases the classification precision and noise heftiness.

Multiple channels LBP (Shu et al., 2021) converts the colour image into a feature vector comprised of inner and intra channel features and local features. Based on colour differences, the sign and magnitude components of the local characteristics are simultaneously retrieved from three channels. The experimental findings have demonstrated, multiple-channel LBP outperforms most of the existing colour texture features in terms of classification precision.

(Bedi et al., 2021) imparted a mean distance local binary pattern for liver ultrasound image retrieval. They apply the concept of the spatial distance of the neighbouring pixels from the neighbourhood center pixel in the local neighbourhood to encode the local binary pattern. They have showed a noteworthy enhancement in the process of retrieving images with the mean distance local binary pattern over existing methods.

(Shu et al., 2022) introduced Global Refined Local Binary Patterns (GRLBP) to categorize the textures. GRLBP is used to define and characterize local neighbourhoods with similar structures but distinct contrasts or gray-scale values. The method employs two descriptors: Center Refined Local Magnitude Binary Pattern (CRLBP_M) and Magnitude Refined Local Sign Binary Pattern (MRLBP_S) to represent texture in the local neighbourhood. The authors have conducted experiments on the Outex, KTH-TIPS, CUReT, UMD, KTH-T2b, UIUC, and DTD datasets, demonstrate that GRLBP offers competitive advantages in classification accuracy, computational efficiency, and feature dimensionality compared to other LBP variants.

A two-layer approach was suggested by (Salih and Abdulla, 2023) to improve the effectiveness of the image retrieval outcomes. Layer 1 uses shape features in the form of a Bag of Features technique to cut down the number of dissimilar images from the image archives. Layer 2 brings out texture features and colour features to retrieve the similar images. The authors have extracted local binary pattern features and wavelet features to represent the texture. The mean and entropy value from each colour channel of three colour spaces are used to represent the colour feature. Similar images are retrieved from the corel-1K database using the combination of extracted features. The authors have come to the conclusion that the two-layer method of content-based image retrieval outperforms the other existing approaches.

(Kumar et al., 2023) presented a layered approach using texture, shape and colour to accelerate the process in the image retrieval system. There are three stages in the layered approach. In stage 1, the similar images are filtered using the Edge Histogram Descriptor shape feature. The second stage process further filters the similar images based on Tamura texture features. The Colour Image Quantization is used to sieve the most similar images in stage 3. Each stage in the layered approach is used to confine the related images from the large dataset. The authors have conducted successful experiments in the Produce-1400, GHIM-10 K, Olivia-2688, and Corel-1 K image archives to retrieve similar images.

A technique for multi-scale averaging local binary patterns was presented by (Fadaei et al., 2024) in order to extract related images from image archives. A feature vector is formed by concatenating the texture features from the various scales of the image. The authors have validated the phenomenal improvement in the retrieval accuracy as compared to the existing CBIR models, especially on the Brodatz, VisTex, Corel-1K, Caltech 256, Corel-10K, Olivia, and STex databases.

(Kumar et al., 2024) applied the fusion of Colour histogram, LBPCd (LBP patterns from the cross product of neighbouring pixels), and Colour difference histogram to represent images for the classification of breast cancer histopathology images. They showed that the fused feature extracted efficiently from the images, and the classification has been proved with the high recognition rate in the BreaKHis and BACH datasets.

It is observed from the review that local binary pattern-based feature extraction methods are proven discriminative and use intensity information within the local neighbourhood based on certain relationships among the pixels. The three relationships are primarily used to derive local patterns: the relationships among the surrounding pixels, the symmetric relationship at the center, and the relationship between the center pixel and its surrounding pixels. No single local pattern incorporates all three types of relationships. Local patterns based on combined relationships give superior performance (Verma et al. (2017)). It is also perceived from the review that the local patterns handle all the neighbouring pixels equally in the local neighbourhood even though the spatial distance of each pixel from the center pixel is different. Further, the relationship of the intensity information in the local neighbourhood is encoded either by the sign component, the magnitude component, or a combination of both. The review shows that local patterns encoded based on the combination of magnitude and sign components are highly superior to the local patterns encoded only by a sign component or a magnitude component. The review has added that the completeness of the local pattern is reached whenever the statistics from the whole image are included in it.

These observations have motivated us to propose a new local pattern named Complete Local Spatial Relationship Pattern (CLSRP) to address the pivotal points of the observations.

1.2 Contributions

This article presents a new discriminative local pattern called the Complete Local Spatial Relationship Pattern (CLSRP) for efficient image retrieval. The following contributions are made to construct the CLSRP local pattern;

i. The CLSRP pattern is constructed by exploiting the relationships between the center pixel and its surrounding pixels, the mutual relationships among the surrounding pixels, and the center-symmetric relationships within the local neighbourhood.

ii. The neighbouring pixels of the central pixel are located at varying spatial distances. Spatially closer neighbouring pixels provide more informative contributions than the more distant ones. In this work, the neighbouring pixels are classified into two groups based on spatial distance, and appropriate weights are assigned to them during the encoding process.

iii. Both the magnitude and the sign components of the relationships are considered when encoding the pattern.

iv. Global mean statistics are incorporated into the local pattern, making the CLSRP descriptor complete.

2. COMPUTATION OF LOCAL PATTERNS USING DIFFERENT RELATIONSHIPS IN THE LOCAL NEIGHBOURHOOD

The computation of the local patterns based on the center pixel and surrounding pixels relationship (relationship 1), such as LBP; the mutual relationship of surrounding pixels (relationship 2), such as LNDP; and the center symmetric relationship (relationship 3), such as CSLBP, in the local neighbourhood are depicted here. A 3X3 neighbourhood is considered for computation.

2.1 Computation of the Local Binary Pattern (LBP)

The LBP exploits the relationship of the middle pixel with neighbouring pixels in the neighbourhood to derive the local pattern. Figure 1 shows the mentioned pixels in the 3X3 tiny local neighbourhood. I_c in Figure 1 represents the intensity (gray) value of the center pixel and I_1, I_2,…, and I_8 represent the intensity (gray) values of neighbouring pixels. The LBP pattern of the pixel with intensity value I_c is computed using (1).

$$\mathrm{LBP}(I_c) = \sum_{i=1}^{8} f_1(I_i - I_c) \times 2^{i-1} \tag{1}$$

The function '$f_1(x)$' in (1) is defined in (2).

$$f_1(x) = \begin{cases} 1 & x \geq 0 \\ 0 & x < 0 \end{cases} \tag{2}$$

$I_1(i-1,j-1)$	$I_2(i-1,j)$	$I_3(i-1,j+1)$
$I_8(i,j-1)$	$I_c(i,j)$	$I_4(i,j+1)$
$I_7(i+1,j-1)$	$I_6(i+1,j)$	$I_5(i+1,j+1)$

Fig. 1. The 3X3 Local Neighbourhood of a Pixel I_c.

Every pixel of the image block MXN is considered as the center pixel and the LBP value is computed. The histogram of the LBP pattern map is utilised to form the feature descriptor of the image. The LBP histogram 'LBPHIST(l)' is computed using (3).

$$LBPHIST(l) = \sum_{i=0}^{M-1} \sum_{j=0}^{N-1} H(LBP(i,j), l); \quad l \in [0, 2^n - 1] \tag{3}$$

The term 'l' represents the length of the histogram. The term 'n' indicates the quantity of neighbouring pixels in the local neighbourhood. Equation (4) defines the function 'H(i,j)' used in (3).

$$H(i,j) = \begin{cases} 1 & i = j \\ 0 & i \neq j \end{cases} \tag{4}$$

2.2 Computation of the Local Neighbourhood Difference Pattern (LNDP)

The LNDP makes use of the mutual relationships between neighbouring pixels in the local neighbourhood to devise the local pattern. The LNDP pattern of the center pixel 'I_c' with reference to the local neighbourhood is determined using (5).

$$LNDP(I_c) = \sum_{i=1}^{8} f_2(I_i) \times 2^{i-1} \tag{5}$$

The function '$f_2(I_i)$' in (5) is portrayed in (6).

$$f_2(I_{i|i=1 \text{ to } 8}) = \begin{cases} 1 & I_{i-1} - I_i \geq 0 \text{ and } I_{i+1} - I_i \geq 0 \\ 1 & I_{i-1} - I_i < 0 \text{ and } I_{i+1} - I_i < 0 \\ 0 & I_{i-1} - I_i \geq 0 \text{ and } I_{i+1} - I_i < 0 \\ 0 & I_{i-1} - I_i < 0 \text{ and } I_{i+1} - I_i \geq 0 \end{cases} \quad \begin{vmatrix} I_{i-1} \text{ for } I_1 \text{ is } I_8 \\ I_{i+1} \text{ for } I_8 \text{ is } I_1 \end{vmatrix} \tag{6}$$

The LNDP pattern is computed for every pixel of the image block MXN. The histogram of the LNDP pattern map represents the image. The LNDP histogram 'LNDPHIST(l)' is configured using (7).

$$LNDPHIST(l) = \sum_{i=0}^{M-1} \sum_{j=0}^{N-1} H(LNDP(i,j), l); \quad l \in [0, 2^n - 1] \tag{7}$$

2.3 Computation of the Center Symmetric Local Binary Pattern (CSLBP)

The CSLBP encodes the relationship of neighbouring pixels that are symmetrically aligned with the center pixel in the local neighbourhood to derive the local pattern. The CSLBP pattern for the center pixel 'I_c' about the local neighbourhood is computed using (8).

$$CSLBP(I_c) = \sum_{i=1}^{4} f_3(I_i) \times 2^{i-1} \tag{8}$$

The function '$f_3(I_i)$' in (8) is defined in (9).

$$f_3(I_{i|i=1 \ to \ 4}) = \begin{cases} 1 & I_{i+4} - I_i \geq 0 \\ 0 & I_{i+4} - I_i < 0 \end{cases} \tag{9}$$

The CSLBP pattern of the image is computed by considering each pixel in the image as the center pixel. The feature descriptive vector of the image is formed from the histogram of the CSLBP pattern map. Equation (10) is used to compute the CSLBP histogram 'CSLBPHIST(l)'.

$$CSLBPHIST(l) = \sum_{i=0}^{M-1} \sum_{j=0}^{N-1} H(CSLBP(i,j), l); \quad l \in [0, 2^4 - 1] \tag{10}$$

3. A PROPOSED FRAMEWORK FOR IMAGE RETRIEVAL USING THE CLSRP PATTERN

This section describes the formation of the suggested image retrieval framework using the CLSRP pattern. The local patterns described in Section 2 leave the magnitude of gray level variations when encoding the patterns in the local neighbourhood and regard the entire neighbouring pixel in the neighbourhood with equal weightage. The proposed CLSRP accounts for the degree of gray level variations besides accounting for the sign of gray level differences in three kinds of pixel relationships, and also applies weightage to the binary pattern of the neighbouring pixels with respect to their spatial distance value from the center pixel. The spatial distance value (Bedi and Sunkaria, 2021) of the neighbouring pixels from the referenced pixel in the pixel grid is presented in Figure 2.

1.44	1	1.44
1	CP	1
1.44	1	1.44

Fig. 2. Spatial distance value of the neighbouring pixels from the center pixel (CP).

The spatial distance value brings a new idea of computing local patterns in the CLSRP from the three relationships mentioned in Section 2. This factor is caused by not treating all the neighbouring pixels uniformly to create the pattern. The neighbouring pixels in the 3X3 neighbourhood given in Figure 1, are partitioned into two groups, where group 1 includes vertical and horizontal neighbours (I_2, I_4, I_6, and I_8) and group 2 comprises diagonal neighbours (I_1, I_3, I_5, and I_7). The pixels that are in group 1 are spatially the closest to the center pixel and are given more weightage than the group 2 pixels while deriving the pattern.

Section 3.1 describes the computation of the CLSRP pattern, and Section 3.2 illustrates the image retrieval methodology using the CLSRP pattern.

3.1 Computation of the proposed CLSRP pattern

The proposed CLSRP pattern has six components. They are as follows: LBP sign (LBP_S), LBP magnitude (LBP_M), LNDP sign (LNDP_S), LNDP magnitude (LNDP_M), CSLBP sign (CSLBP_S), and CSLBP magnitude (CSLBP_M). The global statistics are fused into these components to make the pattern complete. The computations of LBP_S, LBP_M, LNDP_S, LNDP_M, CSLBP_S, and CSLBP_M in the CLSRP are illustrated in the subsections.

3.1.1 Computation of LBP_M and LBP_S patterns based on relationship 1

The LBP_M and LBP_S patterns are computed based on the center pixel and neighbouring pixel relationships in a local neighbourhood. The LBP_S and LBP_M have two sub components, and the subcomponents are computed from grouping of neighbouring pixels with respect to the spatial distance from the center pixel. The LBP_S is computed using (11).

$$\mathrm{LBP\_S}(I_c) = \left[a \times LBP_{S_{hv}}(I_c) + b \times LBP_{S_d}(I_c)\right]$$
$$LBP_{S_{hv}}(I_c) = \textstyle\sum_{i=2,4,6,8} f_4(I_i - I_c) \times 2^{(i-1)/2} \tag{11}$$
$$LBP\_S_d(I_c) = \textstyle\sum_{i=1,3,5,7} f_4(I_i - I_c) \times 2^{i/2}$$

The term ‘LBP_S_{hv}’ describes the LBP sign component derived from the horizontal and vertical neighbours of the local neighbourhood. The term ‘LBP_S_d’ expresses the LBP sign component based on the diagonal neighbours of the local neighbourhood. In a 3X3 neighbourhood, horizontal and vertical neighbours are spatially closer to the center pixel (1 pixel unit) than diagonal neighbours (1.44 pixels unit), hence LBP_Shv has slightly higher weightage (0.6) than LBP_Sd (0.4) to balance their contributions in the descriptor. The values ‘a’ represents the weightage of the horizontal and vertical neighbours, and ‘b’ represents the weightage of the diagonal neighbours. Hence, ‘a’ is assigned to 0.6, and ‘b’ is assigned to 0.4 in this implementation. The function ‘$f_4(x)$’ in (11) is described in (12).

$$f_4(x) = \begin{cases} 1 & \text{if } \mathrm{abs}(x) \geq \mathrm{T} \text{ for LBP\_M } \textit{and} \\ & x \geq \mathrm{T} \text{ for LBP\_S} \\ 0 & \text{if } \mathrm{abs}(x) < \mathrm{T} \text{ for LBP\_M } \textit{and} \\ & x < \mathrm{T} \text{ for LBP\_S} \end{cases} \tag{12}$$

The ‘LBP_M’ is also computed based on (11). The value ‘T’ in (12) for the ‘LBP_S’ component is zero, but for the ‘LBP_M’ component, it is computed using (13).

$$T = \frac{\sum_{i=1}^{8} \mathrm{abs}(I_i - I_c)}{8} \tag{13}$$

The term ‘abs(I_i-I_c)’ in (13) is the absolute gray level variation between the surrounding pixel ‘I_i’ and the center pixel ‘I_c’. Figure 3 explains how the LBP_S and LBP_M patterns are calculated in a sample 3X3 neighbourhood.

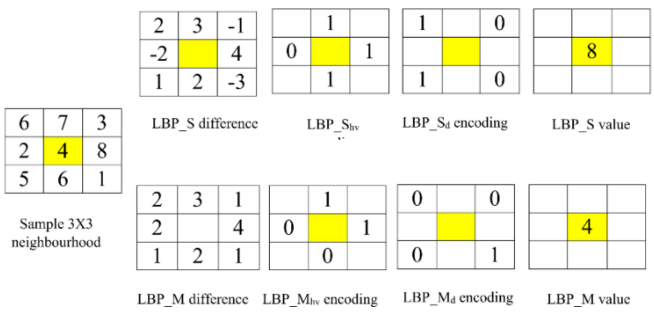

Fig. 3. Computation of the LBP_S and LBP_M patterns based on partitioned neighbouring pixels.

3.1.2 Computation of LNDP_S and LNDP_M patterns based on relationship 2

The LNDP_S and LNDP_M patterns are computed based on the joint association of the neighbouring pixels. The LNDP_S(I_c) is computed using (14).

$$\mathrm{LNDP\_S}(I_c) = \left[a \times LNDP_{S_{hv}}(I_c) + b \times LNDP_{S_d}(I_c)\right]$$
$$LNDP\_S_{hv}(I_c) = \textstyle\sum_{i=2,4,6,8} f_5(I_i) \times 2^{(i-1)/2} \tag{14}$$
$$LNDP\_S_d(I_c) = \textstyle\sum_{i=1,3,5,7} f_5(I_i) \times 2^{i/2}$$

The function ‘$f_5(x)$’ in (14) is depicted in (15).

$$f_5\left(I_{i|i=1 \text{ to } 8}\right) = \begin{cases} 1 & I_{i-1} - I_{i+1} \geq 0 \\ 0 & I_{i-1} - I_{i+1} < 0 \end{cases} \left| \begin{array}{l} I_{i-1} \text{ for } I_1 \text{ is } I_8 \\ I_{i+1} \text{ for } I_8 \text{ is } I_1 \end{array} \right. \tag{15}$$

The LNDP_M(I_c) is computed based on (16).

$$\mathrm{LNDP\_M}(I_c) = \left[a \times LNDP_{M_{hv}}(I_c) + b \times LNDP_{M_d}(I_c)\right]$$
$$LNDP\_M_{hv}(I_c) = \textstyle\sum_{i=2,4,6,8} f_6(I_i) \times 2^{(i-1)/2} \tag{16}$$
$$LNDP\_M_d(I_c) = \sum_{i=1,3,5,7} f_6(I_i) \times 2^{i/2}$$

The function ‘$f_6(x)$’ in (16) is given in (17).

$$f_6\left(I_{i|i=1 \text{ to } 8}\right) = \begin{cases} 1 & \mathrm{abs}(I_{i-1}\text{-}I_{i+1}) \geq T_2 \\ 0 & \mathrm{abs}(I_{i-1}\text{-}I_{i+1}) < T_2 \end{cases} \left| \begin{array}{l} I_{i-1} \text{ for } I_1 \text{ is } I_8 \\ I_{i+1} \text{ for } I_8 \text{ is } I_1 \end{array} \right. \tag{17}$$

The value ‘T_2’ in (17) is evaluated using (18).

$$T_2 = \frac{\sum_{i=1}^{8} \mathrm{abs}(I_{i-1} - I_{i+1})}{8} \quad \left| \begin{array}{l} I_{i-1} \textit{ for } I_1 \textit{ is } I_8 \\ I_{i+1} \textit{ for } I_8 \textit{ is } I_1 \end{array} \right. \tag{18}$$

The term ‘abs(I_{i-1}-I_{i+1})’ in (18) is the absolute gray level difference between the two surrounding pixels of each ‘I_i’. Figure 4 illustrates the computation of LNDP_S and LNDP_M in a unit of 3X3 neighbourhood.

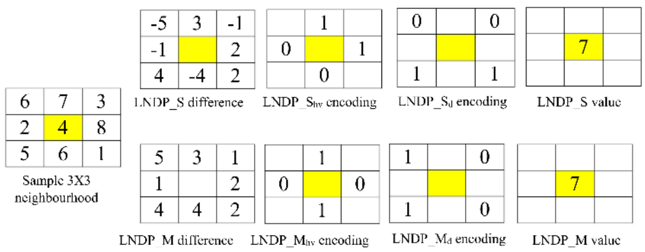

Fig. 4. Computation of LNDP_S and LNDP_M patterns based on partitioned neighbouring pixels.

3.1.3 Computation of CSLBP_S and CSLBP_M patterns based on relationship 3

The CSLBP_S and CSLBP_M patterns are quantified based on the center symmetric relationship in the local neighbourhood. CSLBP_S is computed using (8). Correspondingly, CSLBP_S(I_c)=CSLBP(I_c). The ‘CSLBP_M(I_c)’ is determined using (19).

$$\mathrm{CSLBP\_M}(I_c) = \textstyle\sum_{i=1}^{4} f_7(I_i) \times 2^{i-1} \tag{19}$$

The function ‘$f_7(x)$’ in (19) is delineated using (20).

$$f_7\left(I_{i|i=1 \text{ to } 4}\right) = \begin{cases} 1 & \mathrm{abs}(I_{i+4} - I_i) \geq T_3 \\ 0 & \mathrm{abs}(I_{i+4} - I_i) < T_3 \end{cases} \tag{20}$$

The term ‘T_3’ in (20) is defined using (21).

$$T_3 = \frac{\sum_{i=1}^{4} \mathrm{abs}(I_{i+4} - I_i)}{4} \tag{21}$$

The term ‘abs(I_{i+4}-I_i)’ in (21) is the absolute gray level variation between the center symmetric pixel of ‘I_{i+4}’ and the pixel ‘I_i’.

The histograms of LBP_S, LBP_M, LNDP_S, LNDP_M, CSLBP_S, and CSLBP_M are formed from the pattern maps of the respective components. The global statistics have to be incorporated into any one of these histograms. The global statistics return the image's pattern map with a value of 0 or 1.

The CSLBP looks for only four pairs in the local neighbourhood. The binary value of global thresholding is added as the 5th bit of the CSLBP_M pattern map. Consequently, (19) is modified into (22).

$$\text{Modified CSLBP\_M}(I_c) = \sum_{i=1}^{5} f_7(I_i) \times 2^{i-1} \tag{22}$$

The function ‘f_7’ with values I_1, I_2, I_3, and I_4 is computed using (20) but the function ‘f_7’ with value I_5 is computed with respect to (23).

$$f_7(I_5) = \begin{cases} 1 & if\ local\_mean \geq global\_mean \\ 0 & otherwise \end{cases} \tag{23}$$

The mean gray intensity values in the immediate neighbourhood are referred to as the "local_mean" and the mean gray intensity values for the entire image are referred to as the "global_mean” in (23). The CLSRP pattern histogram of an image is formed by linearly combining the histograms of LBP_S (length of 16 (2^4)), LBP_M (length of 16 (2^4)), LNDP_S (length of 16 (2^4)), LNDP_M (length of 16 (2^4)), CSLBP_S (length of 16 (2^4) and modified CSLBP_M (length of 32 (2^5)).

3.2 The proposed CLSRP pattern based image retrieval Scheme

The proposed work extracts the CLSRP pattern from the image and represents the image for image retrieval task. The working procedure of the image retrieval system using the proposed CLSRP pattern is outlined in Algorithm 1.

The decisive factor in Algorithm 1 is the similarity function that is utilised to find the similar images in database images with reference to query image. The similarity function is defined with the help of the distance metric. Several distance metrics act as the similarity function in image retrieval algorithms. The ‘D1’ distance criterion (Murala et al., 2012; Murala et al., 2012c; Verma et al., 2015) is an excellent similarity function for many image retrieval algorithms that use local patterns as the feature vector. The ‘D1’ distance criterion is given in (24).

The decisive factor in Algorithm 1 is the similarity function that is utilised to find the similar images in database images with reference to query image. The similarity function is defined with the help of the distance metric. Several distance metrics act as the similarity function in image retrieval algorithms. The ‘D1’ distance criterion (Murala et al., 2012; Murala et al., 2012c; Verma et al., 2015) is an excellent similarity function for many image retrieval algorithms that use local patterns as the feature vector. The ‘D1’ distance criterion is given in (24).

$$\text{D1(p,q)} = \sum_{k=0}^{l-1} \left| \frac{p_k - q_k}{1 + p_k + q_k} \right| \tag{24}$$

The term ‘p’ in (24) represents the characteristic vector of the query image, while ‘q’ denotes the characteristic vector of the database image. The value ‘l’ in (24) indicates the length of the characteristic vector.

Algorithm 1 : Scheme of Image Retrieval applying the CLSRP Pattern
Input : An image archive with ‘n’ images, a query image (selected from the image archive), and a decisive factor to define the similarity between the images.
Output : A collection of images from image archive found to be related to the query image.
Step 1 : Input the image database into the image retrieval system and receive the query image from the user.
Step 2 : Form the image representation vector for the query image using the CLSRP histogram.
Step 3 : For k=1 to n
- Step 3.1 : Create the image representation vector of the kth database image using the CLSRP histogram.
- Step 3.2 : Determine the correspondence between the query image’s representation vector and the representation vector of the kth image in the database using a defined decision criterion.
- Step 3.3 : If the value given by the decisive factor is within the threshold, store the kth database image as the relevant image for the given query image.

Step 4 : Output all the relevant images for the given query image.

4. EXPERIMENTAL OUTCOMES AND DELIBERATIONS

This research work proposes the CLSRP pattern for image retrieval applications. Experiments for the image retrieval applications are conducted on the ORL, the UIUC, and the real-world Covid-19 chest X-ray database to manifest the potency of the proposed pattern. There are 400 face images in the ORL database and 1000 texture images in the UIUC database. The Covid-19 database consists of 317 chest X-ray images.

The image retrieval process is executed in line with Algorithm 1. The experimental analysis considers the top ‘n’ output images to determine the efficiency of the image retrieval system. The different values of ‘n’ are taken for performance comparison. The precision and recall metrics (Muller et al., 2001)) that are given in (25) and (26) are used as performance metrics to present retrieval efficiency.

$$\text{Precision} = \frac{\text{No of Relevant images Retrieved}}{\text{Total number of images retrieved}} \tag{25}$$

$$\text{Recall} = \frac{\text{No of Relevant images Retrieved}}{\text{Total number of Relevant images in the database}} \tag{26}$$

Three experiments demonstrate the value of the contemplated work. Experiment 1 is conducted to exhibit the influence of the spatial distance of the neighbourhood pixels on drawing the local patterns based on relationship 1 and relationship 2. Experiment 2 is carried out to present the potency of the work in comparison to other state-of-the-art local patterns in the ORL and UIUC databases. The significance of the CLSRP pattern on the retrieval of the real-world Covid-19 database is demonstrated in experiment 3.

4.1 Experiment 1 (Influence of the spatial distance of the neighbourhood pixels in the local patterns)

This experiment aims to demonstrate the impact of neighbourhood pixel classification based on spatial distance while encoding local patterns. The ORL database is considered for experiment 1. The image retrieval system receives each image as a query from the ORL database. The recall and precision values are analysed separately with respect to the LBP and LNDP. Figure 5 shows the precision analysis of the ORL image retrieval systems using a local binary pattern (LBP_S) and a weighted local binary pattern with partitioned neighbouring pixels (LBP_S_{hv} + LBP_S_d).

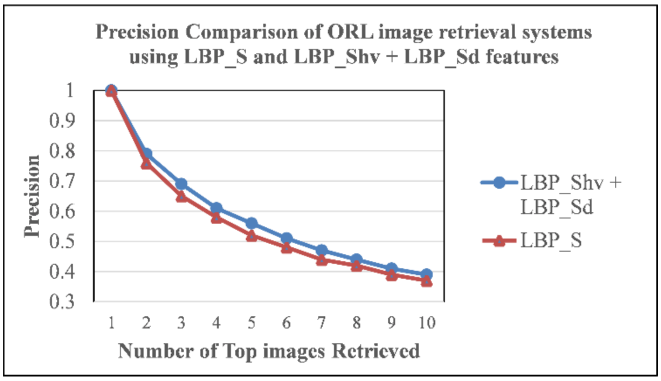

Fig. 5. Precision Comparison of ORL Image Retrieval Systems using LBP_S and LBP_Shv+LBP_Sd features.

It is inferred from Figure 5 that the average precision value of the LBP_S_{hv} + LBP_S_d (0.59) based ORL image retrieval system is higher when compared to the average precision value of the LBP_S (0.52) based ORL image retrieval systems.

Figure 6 depicts a precision analysis of the ORL image retrieval systems using the local neighbourhood difference pattern (LNDP_S) and the weighted local neighbourhood difference pattern with partitioned neighbouring pixels (LNDP_Shv + LNDP_Sd).

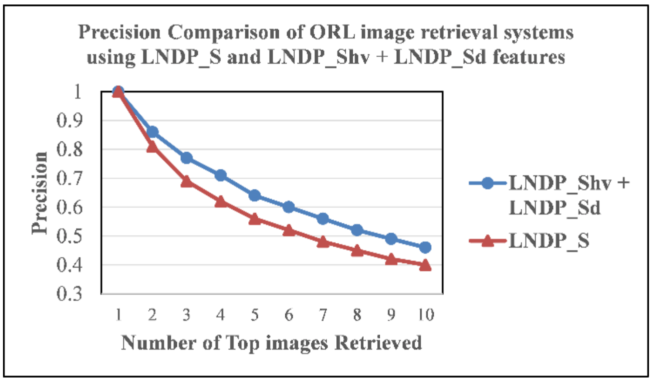

Fig. 6. Precision Comparison of ORL Image Retrieval Systems using LNDP_S and LNDP_Shv+LNDP_Sd features.

The mean precision value of the ORL image retrieval system based on LNDP_Shv + LNDP_Sd (0.76) is increased by 6% as compared to LNDP_S (0.7) based on the comparison given in Figure 6.

Experiment 1 ascertains the improved performance of local patterns by giving weightage to the neighbourhood pixels based on their spatial distance.

4.2 Experiment 2 (Comparative Analysis of the Proposed CLSRP with LTriDP, LNIP, and LBP in Benchmark Databases)

The purpose of this experiment is to prove the eminence of the CLSRP in comparison with other state-of-the-art local patterns. The patterns LTriDP, LNIP, and LBP are considered for the performance comparison. The patterns LTriDP and LNIP are ideal for comparison with CLSRP since both local patterns utilise pixel positions in relationships 1 and 2 in a local neighbourhood and consider both sign and magnitude components. The image retrieval experiment is conducted on the ORL and UIUC databases. The mean precision and recall values are determined using all of the images from the two databases as query images. The maximum number of top images retrieved is considered 10 and 40 respectively, in the ORL and UIUC databases since the ORL database has 10 images in every class and the UIUC database has 40 images in each class. The precision and recall comparisons of the ORL image retrieval systems are given in Figure 7 and Figure 8, respectively.

It is inferred from the mean precision analysis of ORL image retrieval systems that the proposed CLSRP pattern (0.81) outperforms LTriDP, LNIP, and LBP by 18% (0.63), 25% (0.56), and 29% (0.52), respectively.

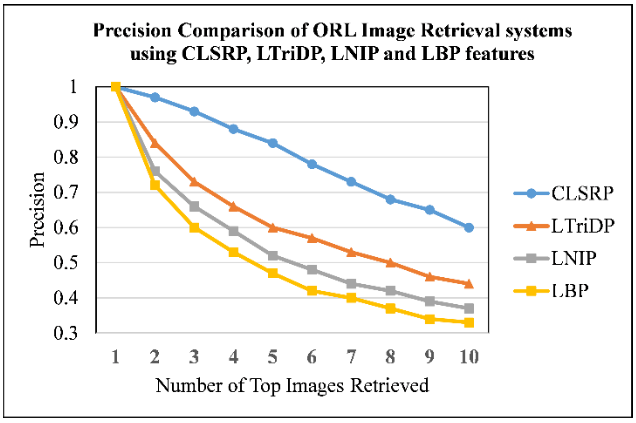

Fig. 7. Precision Comparison of ORL Image Retrieval Systems using CLSRP, LTriDP, LNIP, and LBP Local Patterns for the Top 10 Images Retrieved.

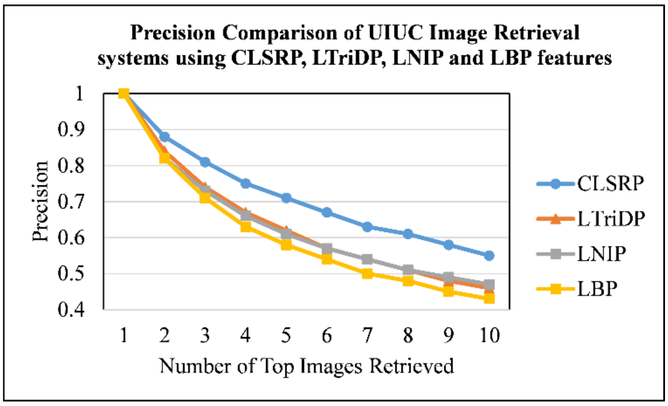

Fig. 8. Recall Comparison of ORL Image Retrieval Systems using CLSRP, LTriDP, LNIP, and LBP Local Patterns for the Top 10 Images Retrieved.

Figure 9 depicts a precision comparison of the retrieval of the Top 10 images in the UIUC image retrieval systems.

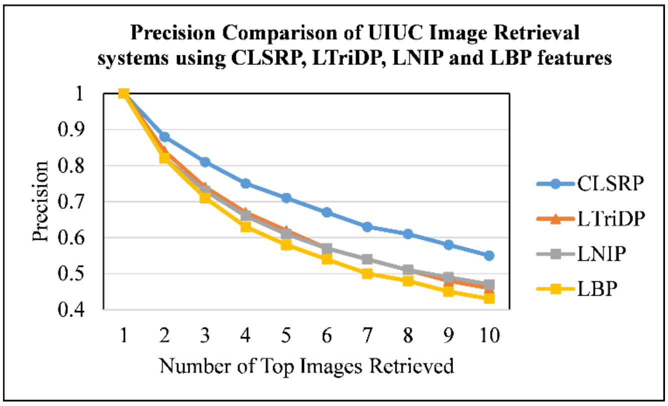

Fig. 9. Precision Comparison of UIUC Image Retrieval Systems using CLSRP, LTriDP, LNIP, and LBP Local Patterns for the Top 10 Images Retrieved.

According to the average precision analysis of UIUC image retrieval systems with respect to the Top 10 images retrieved, the proposed CLSRP pattern (0.72) outperforms LTriDP, LNIP and LBP by 18 % (0.64), 18 % (0.64) and 29% (0.61).

Figures 10 and 11 give the comparative analysis of the UIUC image retrieval systems' precision and recall for the Top 4 retrieved images to the Top 40 retrieved images, respectively.

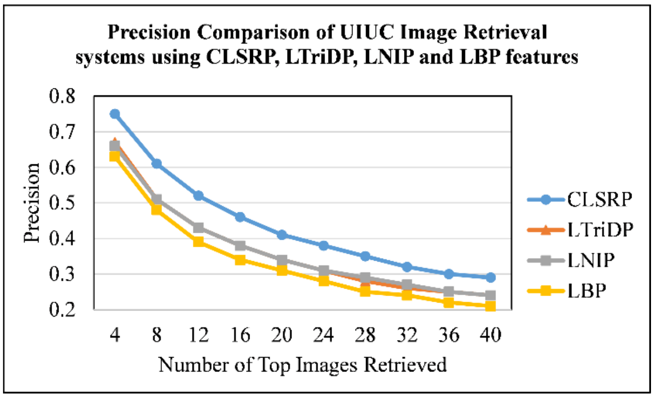

Fig. 10. Precision Comparison of Image Retrieval Systems using CLSRP, LTriDP, LNIP, and LBP Local Patterns for the Top 40 Images Retrieved.

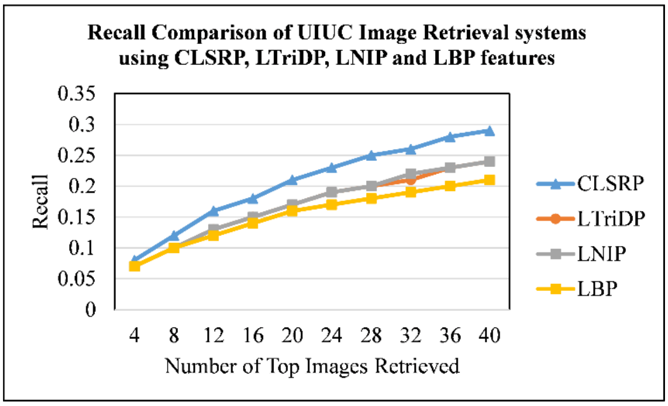

Fig. 11. Recall Comparison of Image Retrieval Systems using CLSRP, LTriDP, LNIP, and LBP Local Patterns for the Top 40 Images Retrieved.

The average precision analysis of UIUC image retrieval systems for the Top 40 images based on CLSRP, LTriDP, LNIP, and LBP patterns reveals that CLSRP (0.44) has an upturn of 7% (0.37) from LTriDP, 7% (0.37) from LNIP, and 10% (0.34) from LBP.

4.3 Experiment 3 (Application of CLSRP in Real-world Covid-19 database for image retrieval)

Experiment 3 is conducted to prove the usefulness of CLSRP in real-world image retrieval. The Covid-19 database used for the classification challenge from Kaggle has been considered for the experimentation. The database consists of 317 images from three classes, namely covid, normal and viral pneumonia. The images in Training and Test are combined for image retrieval applications. The image retrieval process is performed with CLSRP, LTriDP, LNIP, and LBP patterns. The precision and recall analysis are presented in Figure 12 and Figure 13, respectively.

It is apparent from the average precision analysis of the Covid-19 image retrieval systems for the Top 10 images that the CLSRP (0.91) pattern based image retrieval system outstrips LTriDP (0.8) by 11%, LNIP (0.79) by 12%, and LBP (0.65) by 26%.

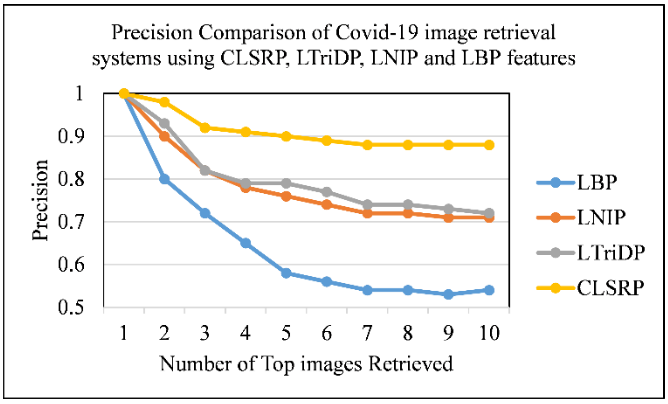

Fig. 12. Precision Comparison of Covid-19 Image Retrieval Systems using CLSRP, LTriDP, LNIP, and LBP Local Patterns for the Top 10 Images Retrieved.

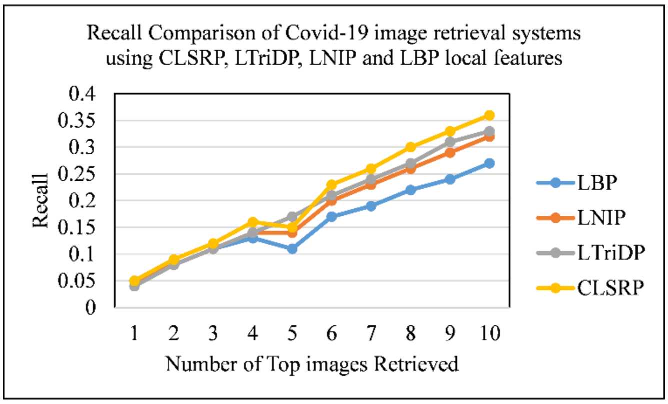

Fig. 13. Recall Comparison of Covid-19 Image Retrieval Systems using CLSRP, LTriDP, LNIP, and LBP Local Patterns for the Top 10 Images Retrieved.

4.4 Length of the Feature (Characteristics) Vector and Computational Complexity

The evaluation of image feature representations considers both feature vector length and computational cost. Computational cost is expressed using asymptotic time complexity to provide an implementation-independent measure of algorithmic efficiency, enabling fair comparison across feature extraction methods. Table 1 presents the feature vector length and computational complexity of local pattern descriptors for a single input image. This representation is well suited for theoretical analysis and scalability assessment, while reporting both measures provides a comprehensive evaluation of feature effectiveness and efficiency.

Table 1. Comparison of Feature vector length and computational complexity

Local Patterns	Feature vector length	Computational Complexity
CLSRP	112	O(N)
LTriDP	768	O(NK)
LNIP	512	O(NK)
LBP	256	O(N)

In Table 1, 'N' denotes the number of image pixels and 'K' the number of neighboring pixels. The complexity O(N) is lower than O(NK), indicating faster feature extraction in practice, which is critical for large-scale and real-time applications. Together with the results of Experiments 2 and 3, the feature vector length and computational cost demonstrate that CLSRP is well suited for image processing and pattern recognition tasks.

4.5 Experimental Discussions

The retrieval efficiency of the local pattern CLSRP from the experiments has been detailed below.

i. The new concept of partitioning neighbourhood pixels with respect to spatial distance in the local neighbourhood is introduced while designing local patterns based on relationship 1 and relationship 2. The experimental evidence for this fact is given in experiment 1 on the ORL database.
ii. The features from all the relationships in the local neighbourhood with sign and magnitude components, including global statistics besides accounting for spatial distance in the local neighbourhood derive CLSRP. The outstanding retrieval efficiency of CLSRP on ORL and UIUC databases is demonstrated in Experiment 2.
iii. The question of the retrieval performance of the suggested CLSRP in a real-world database has been answered in Experiment 3 by applying CLSRP in the Covid-19 chest X-ray dataset. Experiment 3 demonstrated a higher precision value of CLSRP over other state-of-the-art local patterns.
iv. The length of the Feature (characteristics) vector and computational complexity also reinforce the success of the CLSRP pattern.

Experimental results and discussions portray the extortionate efficacy of the CLSRP as compared to other state-of-the-art local patterns.

5. CONCLUSIONS

This work proposes the Complete Local Spatial Relationship Pattern (CLSRP), a very successful local pattern for image retrieval applications. The pattern applies the concept of partitioning neighbourhood pixels in the local neighbourhood based on their spatial distance. Three relationships in the local neighbourhood - the association between the center and neighbouring pixels, the mutual relationship of neighbouring pixels, and the center symmetric relationship are integrated into CLSRP to obtain the local pattern. The sign and magnitude components of all the relationships and the pattern mapping with respect to the global thresholding are stamped into the CLSRP. Experimental evidence from the ORL, UIUC, and real-world Covid-19 chest X-ray databases shows the dominance of CLSRP based image retrieval when compared to state-of-the-art local patterns. This research work suggests that the CLSRP local pattern can be employed to represent the texture for any advanced level image processing applications.

REFERENCES

Banerjee, P. P., Bhunia, A. K., Bhattacharyya, A., Roy, P. P., and Murala, S. (2018). Local Neighborhood Intensity Pattern-A new texture feature descriptor for image retrieval. *Expert Systems with Applications*, 113, 100-115. https://doi.org/10.1016/j.eswa.2018.06.044.

Bedi, A. K., and Sunkaria, R. K. (2021). Mean distance local binary pattern: a novel technique for colour and texture image retrieval for liver ultrasound images. *Multimedia Tools and Applications*, 80, 20773-20802. https://doi.org/10.1007/s11042-021-10758-7.

Christiyana, C. C., and Rajamani, V. (2015). The Complete Local Spatial Central Derivative Binary Pattern for Ultrasound Kidney Images Retrieval. *Applied Medical Informatics*, 37(4), 38-50. https://ami.info.umfcluj.ro/index.php/AMI/article/view/563.

Dubey, S. R., Singh, S. K., and Singh, R. K. (2015). Local diagonal extrema pattern: a new and efficient feature descriptor for CT image retrieval. *IEEE Signal Processing Letters*, 22(9), 1215-1219. DOI:10.1109/LSP.2015.2392623.

Fadaei, S., Dehghani, A., and Ravaei, B. (2024). Content-based image retrieval using multi-scale averaging local binary patterns. *Digital Signal Processing*, 146, 104391. https://doi.org/10.1016/j.dsp.2024.104391.

Fekri, S., and Ershad. (2020). Bark Texture Classification using Improved Local Ternary Patterns and Multilayer Neural Network. *Expert Systems with Applications*, 158, 113509. https://doi.org/10.1016/j.eswa.2020.113509.

Guo, Z., Zhang, L., and Zhang, D. (2010). A completed modeling of local binary pattern operator for texture classification. *IEEE Transactions on Image Processing*, 19(6), 1657-1663. DOI:10.1109/TIP.2010.2044957.

Hafiane, A., Seetharaman, G., and Zavidovique, B. (2007). Median binary pattern for textures classification. *In Proceedings of the 4th International Conference on Image Analysis and Recognition (ICIAR 2007), Lecture Notes in Computer Science*, 4633, 387-398. https://doi.org/10.1007/978-3-540-74260-9_35.

Haralick, R. M., Shanmugam, K., and Dinstein, I. (1973). Textural features for image classification. *IEEE Transactions on Systems, Man, and Cybernetics: Systems*, 3(6), 610-621. https://doi.org/10.1109/TSMC.1973.4309314.

He, Y., and Sang, N. (2011). Robust illumination invariant texture classification using gradient local binary patterns. *In Proceedings of 2011 International Workshop on Multi-Platform/Multi-Sensor Remote Sensing and Mapping, Xiamen, China, January 10-12*, 1-6. DOI:10.1109/M2RSM.2011.5697422.

Heikkila, M., Pietikainen, M., and Schmidb, C. (2009). Description of interest regions with local binary patterns. *Pattern Recognition*, 42(3), 425-436. https://doi.org/10.1016/j.patcog.2008.08.014.

Jin, H., Liu, Q., Lu, H., and Tong, X. (2004). Face detection using improved LBP under bayesian framework. *In Proceedings of 3rd International Conference on Image and Graphics, ICIG 2004, Hong Kong, China, December 18-20*, 306-309. DOI:10.1109/ICIG.2004.62.

Kas, M., Khadiri, I. E., Merabet, Y. E., Ruichek, Y., and Messoussi, R. (2020). Multi Level Directional Cross Binary Patterns: New handcrafted descriptor for SVM-based texture classification. *Engineering Applications of Artificial Intelligence*, 94, 103743. https://doi.org/10.1016/j.engappai.2020.103743.

Kumar, A., Singh, C., and Sachan, M. K. (2024). A novel cross correlation-based colour texture descriptor for the classification of breast cancer histopathology images. *Biomedical Signal Processing and Control*, 93, 106157. https://doi.org/10.1016/j.bspc.2024.106157.

Kumar, S., Pal, A. K., Varish, N., Nurhidayat, I., Eldin, S. M., and Sahoo, S. K. (2023). A hierarchical approach based CBIR scheme using shape, texture, and colour for accelerating retrieval process. *Journal of King Saud University Computer and Information Sciences*, 35(7), 101609. https://doi.org/10.1016/j.jksuci.2023.101609.

Liao, S., Law, M. W. K., and Chung, A. C. S. (2009). Dominant local binary patterns for texture classification. *IEEE Transactions on Image Processing*, 18(5), 1107-1118. DOI:10.1109/TIP.2009.2015682.

Liu, L. L., Chen, J., Fieguth, P., Zhao, G., Chellappa, R., and Pietikainen, M. (2019). From BoW to CNN:Two Decades of Texture Representation for Texture Classification. *International Journal of Computer Vision*, 127, 74-109. https://doi.org/10.1007/s11263-018-1125-z.

Liua, Y., Zhang, D., Lu, G., and Ma, W. Y. (2007). A survey of content-based image retrieval with high-level semantics. *Pattern Recognition*, 40(1), 262-282. https://doi.org/10.1016/j.patcog.2006.04.045.

Loupias, E., Sebe, N., Bres, S., and Jolion, J. -M. (2000). Wavelet-based salient points for image retrieval. *In Proceedings of the IEEE 7th International Conference on Image Processing, ICIP 2000, Vancouver, BC, Canada, September 10-13*, 518-521. DOI:10.1109/ICIP.2000.899469.

Mahesh, D. B., Murty, G. S., and Lakshmi, D, R. (2021). Optimized Local Weber and Gradient Pattern-based medical image retrieval and optimized Convolutional Neural Network-based classification. *Biomedical Signal Processing and Control*, 70, 102971. https://doi.org/10.1016/j.bspc.2021.102971.

Manjunath, S., and Ma, W. Y. (1996). Texture features for browsing and retrieval of image data. *IEEE Transactions on Pattern Analysis and Machine Intelligence*, 18(8), 837-842. DOI: 10.1109/34.531803.

Muller, H., Muller, W., Squire, D. M., Marchand-Maillet, S., and Pun, T. (2001). Performance evaluation in content-based image retrieval: overview and proposals. *Pattern Recognition Letters*, 22(5), 593-601. https://doi.org/10.1016/S0167-8655(00)00118-5.

Murala, S., Maheshwari, R. P., and Balasubramanian, R. (2012a). Directional local extrema patterns: a new descriptor for content-based image retrieval. *International Journal of Multimedia Information Retrieval*, 1, 191-203. https://doi.org/10.1007/s13735-012-0008-2.

Murala, S., Maheshwari, and R. P., Balasubramanian, R. (2012b). Local maximum edge binary patterns: a new descriptor for image retrieval and object tracking. *Signal Processing*, 92(6), 1467-1479. https://doi.org/10.1016/j.sigpro.2011.12.005.

Murala, S., Maheshwari, R. P., and Balasubramanian, R. (2012c). Local tetra patterns: a new feature descriptor for content-based image retrieval. *IEEE Transactions on Image Processing*, 21(5), 2874-2886. DOI:10.1109/TIP.2012.2188809.

Nanni, L., Lumini, A., and Brahnam, S. (2010). Local binary patterns variants as texture descriptors for medical image analysis. *Artificial Intelligence in Medicine*, 49(2), 117-125. https://doi.org/10.1016/j.artmed.2010.02.006.

Ojala, T., Pietikainen, M., and Harwood, D. (1996). A comparative study of texture measures with classification based on featured distributions. *Pattern Recognition*, 29(1), 51-59. https://doi.org/10.1016/0031-3203(95)00067-4.

Pan, Z., Hu, S., Wu, X., and Wang, P. (2021). Adaptive center pixel selection strategy in Local Binary Pattern for texture classification. *Expert Systems with Applications*, 180, 115123. https://doi.org/10.1016/j.eswa.2021.115123

Qian, X., Hua, X., Chen, P., and Ke, L. (2011). PLBP: An effective local binary patterns texture descriptor with pyramid representation. *Pattern Recognition*, 44(10-11), 2502-2515. https://doi.org/10.1016/j.patcog.2011.03.029.

Reddy, P. V. B., and Reddy, A. R. M. (2014). Content based image indexing and retrieval using directional local extrema and magnitude patterns. *AEU – International Journal of Electronics and Communications*, 68(7), 637-643. https://doi.org/10.1016/j.aeue.2014.01.012.

Salih, F. A. A., and Abdulla, A. A. (2023). Two-layer content-based image retrieval technique for improving effectiveness. *Multimedia Tools and Applications*, 82, 31423–31444. https://doi.org/10.1007/s11042-023-14678-6.

Shu, X., Pan, H., Shi, J., Song, X., and Wu, X. (2022). Using global information to refine local patterns for texture representation and classification. *Pattern recognition*, 131, 108843. https://doi.org/10.1016/j.patcog.2022.108843.

Shu, X., Song, Z., Shi, J., Huang, S., and Wu, X. J. (2021). Multiple channels local binary pattern for colour texture representation and classification. *Signal Processing: Image Communication*, 98, 116392. https://doi.org/10.1016/j.image.2021.116392.

Sukhia, K. N., Riaz, M. M., Ghafoor, A., and Ali, S. S. (2020). Content-based remote sensing image retrieval using multi-scale local ternary pattern. *Digital Signal Processing*, 104, 102765. https://doi.org/10.1016/j.dsp.2020.102765.

Sumana, I. J., Islam, M. M., Zhang, D., and Lu, G. (2008). Content based image retrieval using curvelet transform. *In Proceedings of the IEEE 10th Workshop on Multimedia Signal Processing, Cairns, Queensland, Australia, October 8-10*, 11-16. DOI:10.1109/MMSP.2008.4665041.

Tamura, H., Mori, S., and Yamawaki, T. (1978). Textural features corresponding to visual perception. *IEEE Transactions on Systems, Man, and Cybernetics: Systems*, 8(6), 460-473. https://doi.org/10.1109/TSMC.1978.4309999.

Tan, X., and Triggs, B. (2010). Enhanced Local Texture Feature Sets for Face Recognition Under Difficult Lighting Conditions. *IEEE Transactions on Image Processing*, 19(6), 1635-1650. DOI:10.1109/TIP.2010.2042645.

Tian, D. P. (2013). A Review on Image Feature Extraction and Representation Techniques. *International Journal of Multimedia and Ubiquitous Engineering*, 8(4), 385-396. https://www.earticle.net/Article/A202352.

Verma, M., and Raman, B. (2015). Center symmetric local binary co-occurrence pattern for texture, face and bio-medical image retrieval. *Journal of Visual Communication and Image Representation*, 32, 224-236. https://doi.org/10.1016/j.jvcir.2015.08.015.

Verma, M., and Raman, B. (2016). Local tri-directional patterns: A new texture feature descriptor for image retrieval. *Digital Signal Processing*, 51, 62-72. DOI:10.1016/j.dsp.2016.02.002.

Verma, M., and Raman, B. (2017). Local neighborhood difference pattern: A new texture feature descriptor for natural and texture image retrieval. *Multimedia Tools and Applications*, 77(10), 11843-11866. DOI:10.1007/s11042-017-4834-3.

Xia, Y., Wan, S., and Yue, L. (2014). Local spatial binary pattern: A new feature descriptor for content-based image retrieval. *In Proceedings of 5th International conference on graphic and image processing, ICSIP 2014, Bangalore, India, January 8-10*, 9069. https://doi.org/10.1117/12.2049916.

Xu, X., Li, Y., and Wu, Q. M. J. (2020). A completed local shrinkage pattern for texture classification. *Applied Soft Computing*, 97, 106830. https://doi.org/10.1016/j.asoc.2020.106830.

Zhang, B., Gao, Y., Zhao, S., and Liu, J. (2010). Local derivative pattern versus local binary pattern: face recognition with high-order local pattern descriptor. *IEEE Transactions on Image Processing*, 19(2), 533-544. DOI:10.1109/TIP.2009.2035882.

Zhang, D., Islam, M. M., and Lu, G. (2012). A review on automatic image annotation techniques. *Pattern Recognition*, 45(1), 346-362. https://doi.org/10.1016/j.patcog.2011.05.013.